Thermochimica Acta 736 (2024) 179744

Contents lists available at ScienceDirect

Thermochimica Acta

journal homepage: www.elsevier.com/locate/tca

Time-temperature-transformation diagrams from isoconversional kinetic analyses applied to the processing and reprocessing of vitrimers

D. Sanchez-Rodriguez [a,b], S. Zaidi [a,b], L. Carreras [a], Alaitz Ruiz de Luzuriaga [c], Alaitz Rekondo [c], J. Costa [a], J. Farjas [a,b,*]

[a] AMADE - Analysis and Advanced Materials for Structural Design, Polytechnic School, University of Girona, C/ Universitat de Girona 4, E-17003 Girona, Spain
[b] GRMT Materials Research Group and Thermodynamics, Polytechnic School, University of Girona, C/ Universitat de Girona 4, E-17003 Girona, Spain
[c] CIDETEC, Basque Research and Technology Alliance (BRTA), Po. Miramón 196, 20014 Donostia-San Sebastián, Spain

ARTICLE INFO

Keywords:
Isoconversional analysis
Time-temperature-transformation diagrams
Vitrimer
Thermoset
Curing kinetics
Stress relaxation kinetics

ABSTRACT

In this study, we extend the application of Time-Temperature-Transformation (TTT) diagrams, typically employed to describe thermoset processing, to address both the processing and reprocessing of vitrimers. To that end, we have used thermal analysis methods to characterize the reactions governing curing and the thermoforming of a disulfide-containing epoxy vitrimer. The resulting diagrams, which account for adverse processing effects such as degradation and vitrification, exclusively rely on predictions derived from isoconversional methods. Notably, we introduce, for the first time, the application of isoconversional methods to the modeling of stress relaxation kinetics. Using these diagrams, we have identified the conditions for safe curing and thermoforming of the vitrimer. Predictions have been experimentally validated, confirming the robustness and versatility of model-free kinetic analyses.

1. Introduction

The use of polymers for component design is wide-spread across all engineering disciplines [1]. New formulations are constantly emerging to fine-tune specific properties such as toughness, resilience, strength, or transparency, to meet a range of application requirements. Traditionally, thermosets have been the choice for demanding applications as they offer superior chemical resistance, thermal stability, and mechanical properties compared to thermoplastic materials [2]. However, because of the current climate emergency scenario society is shifting towards sustainable materials, an attribute current thermoset do not have [3]. This shift has led to the development of novel types of thermoset-like polymers based on the covalent adaptable network (CAN) concept [4]. CANs differ from thermosets in that the former contain dynamic covalent bonds in the polymer network. Consequently, because CANs have the ability to change their topology they can be reshaped and repaired [5]. Among CANs, vitrimers stand out because they maintain their cross-linking connectivity at all times through associative exchange reactions, allowing their macroscopic properties to be preserved during reprocessing [6–8]. However, achieving exceptional performance is of no use if two fundamental characteristics are not fulfilled: processability and low cost. In fact, these two features are interconnected, with the cost of a product being influenced by the processing conditions.

The idea of generating a state diagram to assist with deciding on the processing conditions is not new and has been embodied in the so-called Time-Temperature-Transformation (TTT) diagrams [9–15]. In the case of thermosets, TTT diagrams are used to illustrate the kinetics of the main phenomena involved in the curing process: gelation and vitrification. TTT diagrams can also be extended to vitrimer processing without one having to take any further considerations into account. On the other hand, the reprocessing of vitrimers is dictated by different kinetic processes that require a reinterpretation of the concept leading to a different type of state diagram. We recently proposed a novel TTT diagram for reprocessing vitrimers that takes into account the kinetics of their characteristic exchange reaction [13].

TTT plots are generated using thermal analysis methods which allow one to obtain experimental points of the diagram and, also, to predict them using kinetic models. Kinetic methods can be classified as model-fitting or model-free. The former assume that the kinetics follows a certain reaction model. Mechanistic models, based on an elaborate theoretical and experimental analysis, can be used to describe the

* Corresponding author.
E-mail address: jordi.farjas@udg.edu (J. Farjas).

https://doi.org/10.1016/j.tca.2024.179744
Received 31 January 2024; Received in revised form 1 April 2024; Accepted 2 April 2024
Available online 3 April 2024

evolution of the cure process. This is often an arduous task requiring expertise in various advanced techniques and a time-consuming multi-parameter fitting of a set of non-analytical expressions. Alternatively, the cure reaction in thermosets can be described by phenomenological reaction models that take into account the autocatalytic nature of the process. Most typically, researchers rely on empirical expressions [15–17] such as that proposed by Kamal [16]. Describing the reaction rate with such simplified expressions carries the risk of not correctly describing the evolution of the systems in which the kinetics deviates from these models.

Conversely, model-free methods are more versatile since they are not tied to a particular reaction pathway. In addition, the assumption that the state of the system is exclusively defined by the degree of transformation seems to hold for resin systems used in industry [18–28]. In fact, this is the same principle that underlies the so-called isoconversional methods, which provide accurate predictions over a temperature range relevant for practical purposes.

In this study, we generate TTT processing and reprocessing diagrams of a vitrimer, based solely on predictions derived from isoconversional methods. A novel aspect of our study is the first-time application of this analytical approach to study the stress relaxation of vitrimers. To construct the diagrams we use a vitrimer based on aromatic disulfide bonds, which has properties that are particularly interesting for the manufacture of composite laminates. The objective of this work is to discuss and validate the applicability of isoconversional methods in generating such isothermal state diagrams.

2. Experimental details and methods

2.1. Kinetic methods

Thermal analysis (TA) is a set of techniques that allow a particular material property to be monitored when a sample is subjected to a controlled temperature program. TA is therefore useful for characterizing the kinetics of processes that occur during thermal treatment.

For example, DSC allows the evolution of heat to be monitored. Thus, DSC has been widely used to analyze the cure kinetics of resins. The cure rate can be determined by DSC by assuming that the degree of cure is proportional to the heat released during the cure process [29]:

$$\frac{d\alpha}{dt} = \frac{1}{\Delta H}\frac{dH}{dt} \tag{1}$$

TGA is also particularly suitable for characterizing degradation kinetics because it monitors the evolution of mass. In this case, it is generally assumed that the degree of degradation is linearly dependent on the mass:

$$\alpha(t) = \frac{m_i - m(t)}{m_i - m_f}, \tag{2}$$

where m_i and m_f are the initial and final masses, respectively.

Isoconversional methods are based on the hypothesis that, for a given degree of conversion α, the conversion rate is only a function of temperature [30,31]:

$$\left[\frac{d\ln(d\alpha/dt)}{dT^{-1}}\right]_\alpha = -\frac{E_\alpha}{R}, \tag{3}$$

where T is the temperature, R the universal gas constant and E_α is the activation energy at a given degree of conversion. In most real thermally activated processes, the microscopic energy barriers remain almost constant as the transformation proceeds [32]. In the case of complex transformations, the dependence of E_α on α is the result of the involvement of different processes, each associated with a particular activation energy, or the involvement of processes that do not obey the Arrhenius dependence of the rate constant on temperature [19,20,33]. Hence, in general, E_α must be interpreted as an apparent activation energy rather than an actual activation energy.

The transformation rate equation can be obtained from the integration of Eq. (3):

$$\frac{d\alpha}{dt} = A_\alpha f(\alpha)\exp\left[-\frac{E_\alpha}{RT}\right]. \tag{4}$$

For a given degree of conversion, the conversion rate is fully described by two parameters: the apparent activation energy E_α, and the product $A_\alpha f(\alpha)$.

The aim of isoconversional methods is, therefore, to determine these two parameters as a function of the degree of conversion. For this purpose, the degree of transformation is discretized into small and constant intervals; $\alpha_j = j\Delta\alpha$. Thus, the objective is to determine the discrete set of values E_j and $Af(\alpha)|_j$. To do this, one must perform several experiments [34,35] at different heating rates, $\beta \equiv dT/dt$ (non-isothermal) or fixed temperatures (isothermal). For example, Friedman's differential isoconversional method is based on a relationship derived directly from Eq. (4):

$$\ln\left(\frac{d\alpha}{dt}\right)_{j,i} = -\frac{E_j}{RT_{j,i}} + \ln(Af(\alpha))|_j \tag{5}$$

where the subscript i stands for a particular experiment, β_i for non-isothermal or T_i for isothermal and the subscript j stands for a given degree of transformation α_j. More precisely, for each heating rate and for a given α_j we determine the transformation rate, $d\alpha/dt|_{j,i}$, and the associated temperature, $T_{j,i}$. According to Equation 5, the plot of $\ln\left(\frac{d\alpha}{dt}\right)_{j,i}$ against the reciprocal of the temperature should give a straight line. The parameter E_j and the product $Af(\alpha)|_j$ are obtained from the slope and intercept, respectively.

Once we know E_j and $Af(\alpha)|_j$, and from the integration of Eq. (4), we can easily make isothermal predictions:

$$\Delta t = \int_{\alpha_m}^{\alpha_{m+n}} \frac{\exp\left[\frac{E_\alpha}{RT}\right]}{Af(\alpha)}d\alpha \tag{6}$$

where T is the constant temperature, Δt is the time span between the degrees of transformation α_m and α_{m+n}, and $\alpha_{m+n} - \alpha_m = n\Delta\alpha$, i.e. the calculated values of the degree of transformation follow the same discretization used to determine the kinetic parameters. Since the integration is computed at equally spaced values of α, we have used the closed Newton-Cotes Bode's formula ($n = 5$) [36].

Besides, the Roduit method [37,38] can be adapted to work for an arbitrary temperature program [13,39]. In this case, the dependence of the temperature with time is given by a discrete set of values $T_k = T(t_k)$. The prediction is based on the summation of Eq. (4) over small time intervals, Δt_k:

$$\alpha_{k+1} = \alpha_k + Af(\alpha)|_k \cdot e^{-\frac{E_k}{RT}}\,\Delta t_k \tag{7}$$

where α_k, E_k and $Af(\alpha)|_k$ are α, E_α and $A_\alpha f(\alpha)$ for a given temperature T_k and Δt_k is the time span between T_k and T_{k+1}. Thus, the evolution of the degree of transformation is obtained iteratively starting from $k = 0$ and $\alpha_0 = 0$.

2.2. Material and thermal analysis techniques

The vitrimer examined in this study is formulated with Araldite XB 6469 (E.E.$W = 150$ g/eq.), a low-viscosity commercial epoxy resin from Huntsman (Duxford, UK), which is a combination of two difunctional epoxies: DGEBA (> 70 %; < 90 %) and 4-Butanediol diglycidyl ether (> 10 %; < 30 %). Additionally, it incorporates an aromatic disulfide hardener, 4-Aminophenyl disulfide (CAS number 722–27–0), which provides dynamic cross-linking capabilities. The epoxy-hardener mixture was prepared at a ratio of 40 phr (parts of hardener per 100

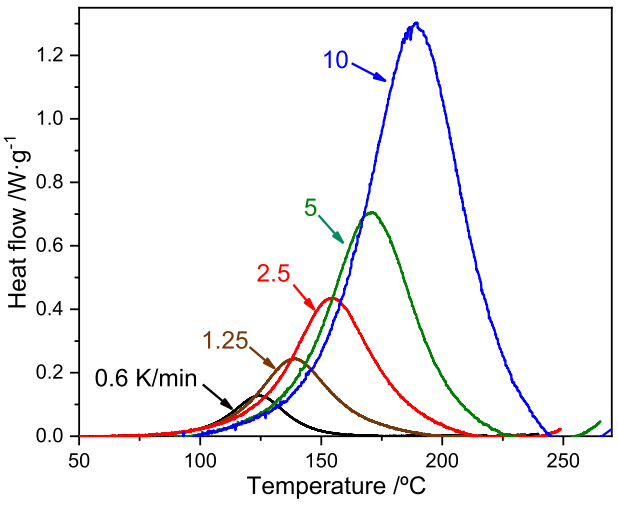

Fig. 1. Non-isothermal DSC analysis of the vitrimer heated at different rates.

parts of resin) as instructed by CIDETEC, who hold a patent for this formulation.

The curing reaction kinetics of the vitrimeric resin were investigated through DSC, employing a Q2000 apparatus from TA Instruments. The analysis was conducted at five distinct heating rates: 0.6, 1.25, 2.5, 5 and 10 K/min. The experiments were carried out in sealed aluminum T-zero pans under a high-purity nitrogen flow rate of 50 ml/min, and the tests were initiated immediately after the resin-hardener mixing to prevent any substantial transformation prior curing. Gelation and vitrification kinetics, crucial to the curing process of thermosets and vitrimers, were indirectly characterized through the modeling of cure reaction and by establishing the gel point-conversion and Tg-conversion relationships.

Gelation at several temperatures has been determined by the cross-over point between the elastic modulus (G') and viscous modulus (G''), in accordance with the methodology proposed elsewhere [40,41]. Four isothermal tests were conducted at temperatures ranging from 100 to 140 °C using an Anton Paar rheometer, model MCR 302e, equipped with an environmental chamber to control the temperature during the experiments. The uncured sample was positioned between 25 mm diameter aluminum disposable parallel plates and subjected to a rotational oscillation test with a constant shear strain of 5 % at a frequency of 1 Hz. Throughout the experiments, the gap (distance between plates) was consistently maintained at 1 mm.

The evolution of the glass transition temperature (Tg) with the degree of cure was analyzed by means of DSC tests. To explore the correlation between the degree of cure and the glass transition temperature, various samples were subjected to different temperature programs leading to distinct levels of conversion. The degree of cure is determined using Eq. (7) and the temperature-time evolution recorded by the DSC. We have summarized in Table S1 the temperature history of such tests along with the predicted degree of conversion. The Tg is determined following the established methodology [42]; the midpoint between the extrapolated onset and endset transition temperatures.

The kinetics of the exchange reaction enabling the reprocessing of vitrimeric resins were characterized through dynamic mechanical analysis using a DMA Q800 instrument via stress-relaxation tests. These tests involve applying a fixed deformation to a specimen and measuring the load required to maintain a constant deformation. Specifically, stress-relaxation experiments were conducted under tensile mode following the methodology established in [43]: fully cured specimens were preloaded at a force of 1×10^{-3} N for straightness, allowing 30 min for thermal equilibrium after reaching the testing temperature. The samples were then stretched by 1 %, and the subsequent stress decrease was recorded to calculate the stress relaxation modulus.

Finally, dynamic TGA was conducted using a Mettler Toledo thermobalance (model TGA/DSC1) to study thermal decomposition kinetics. Like the dynamic calorimetric experiments, we also performed experiments at five different heating rates: 1.25, 2.5, 5, 10, and 20 K/min, under a flow rate of 60 ml/min of high purity synthetic air and at 1.25, 2.5, 5 and 20 K/min, under a flow rate of 60 ml/min of high purity N_2. All tests were conducted using 150 μL Al_2O_3 crucibles, and the sample mass was kept below 5 mg to ensure a negligible effect of overheating on the degradation kinetics [44].

Table 1
Enthalpies of reaction determined from the integration over time of the DSC curves shown in Fig. 1.

Heating rate [K/min]	ΔH [kJ/kg]	ΔH per eq. of epoxy [kJ/eq]
0.60	367	77.1
1.25	382	80.2
2.50	385	80.9
5.0	380	79.8
10.0	386	81.1
Average	380 ± 4	79.8 ± 0.7

3. Results and discussion

3.1. Curing kinetics

Like thermosets, the transformation of a vitrimer into a stable three-dimensional polymeric matrix involves the chemical reaction between the resin and the hardener. Therefore, a thorough understanding of the kinetics of this reaction is fundamental for the optimization of vitrimer's processing. This section aims to characterize cure kinetics through thermal analysis experiments.

Fig. 1 illustrates the dynamic DSC analysis of the curing reaction. The enthalpy of reaction for each experiment is given in table 1. Within the accuracy of the DSC we obtain a constant value of the enthalpy (relative deviations are around 1 %), so that for all DSC experiments a full degree of cure is achieved. The measured enthalpy normalized per epoxy functionality, at 79.8 kJ/mol, is slightly lower than that of other aromatic epoxy-amine systems, which typically fall around 100 kJ/mol [45–47]. The behavior of this resin closely mirrors that of a previously studied vitrimer based on a different epoxy resin but cured with the same hardener [13]. Notably, both exhibit a single exothermic peak in the 100–270 °C temperature range. Additionally, one can observe the initiation of a second exothermic process at temperatures around 250 °C. This is not coincidental, as it corresponds to the higher temperatures that limit the thermal stability of the disulfide bonds of the hardener [13].

To characterize the kinetics of the reaction, we applied Friedman's isoconversional analysis to the experimental data shown in Fig. 1. Fig. 2 shows the dependence of the apparent activation energy, E_α, on the degree of cure along with the correlation coefficient of the linear fitting, demonstrating a good fit over the entire conversion range. The evolution of E_α with α is also not far from that shown by other epoxy-amine systems [14,15,48–50]; it shows a high value at very low conversions that corresponds to the primary amine addition. Then, due to the hydroxyl groups formed during the reaction, the process becomes autocatalytic and the activation energy decreases very rapidly to a relatively constant value around 56 kJ/mol. This low activation energy is similar to that reported for other epoxy-based resins [50,51] and it is in agreement with the activation energy of 58 kJ/mol determined for an epoxy vitrimer [52].

To check the isoconversional fit, we performed a self-consistency test consisting in calculating the evolution of the curing conversion with time for the experiments used in the isoconversional analysis, and the result is represented in Fig. 2.b as continuous lines. To make this prediction we use Eq. (7), where T(t) is the temperature-time evolution extracted from the experimental curves. From Fig. 2.b it is clear that the kinetic analysis correctly predicts the measured evolution for the non-

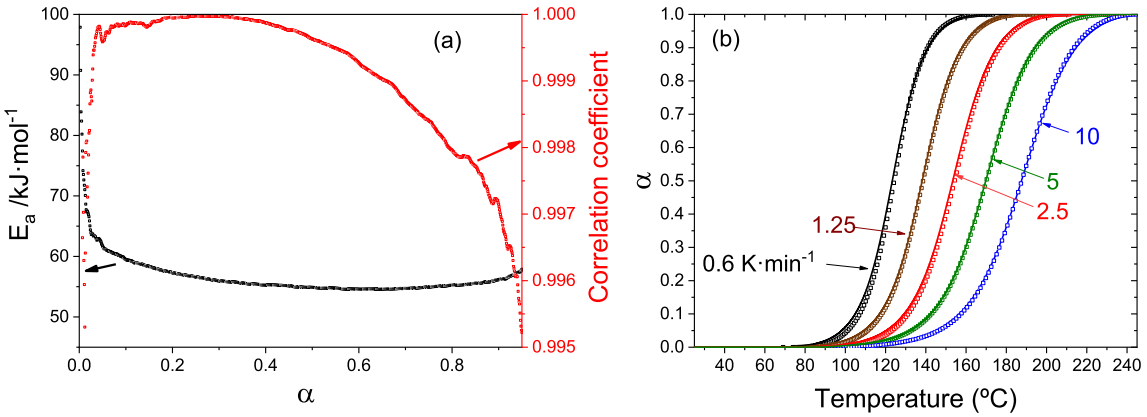

Fig. 2. (a) Apparent activation energy of the curing reaction determined using Friedman isoconversional analysis (left-side axis), together with the correlation coefficient of the linear fitting (right-side axis). (b) Evolution of the degree of curing obtained from the DSC (symbols) and the related prediction using Eq. (7) (solid lines).

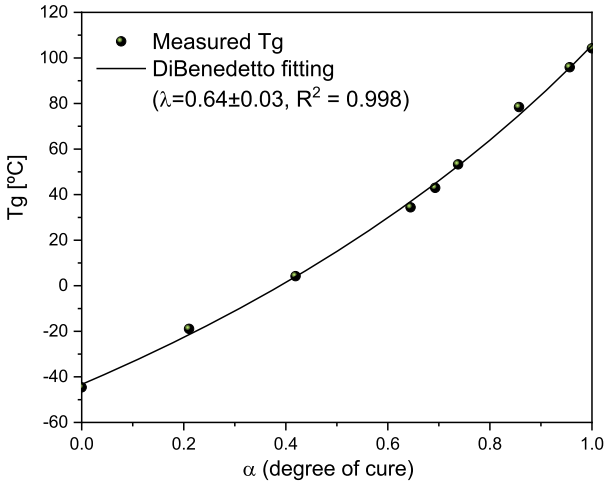

Fig. 3. Symbols: Experimental measurements of the glass transition temperature, Tg, for samples cured up to different conversion degrees. Line: Fitting of the Tg-conversion relationship using the DiBenedetto equation.

isothermal experiments.

While the kinetic characterization in Fig. 2 is able to perfectly describe the non-isothermal curing of the resin, it has its limitations when extended to isothermal curing. This is because the reaction becomes limited by diffusion as the glass transition temperature (Tg) approaches the processing temperature. This phenomenon is known as vitrification. To overcome this, it is essential to identify the dependence of Tg on the curing degree. Notice that the α-Tg relationship also denotes the maximum fractional conversion predictable by our isoconversional model, α_{max}, at that specific temperature [18]. In this study, we do not characterize the kinetics beyond α_{max}, as this region loses relevance from a processing point of view.

We have experimentally determined the Tg for samples cured to different degrees of conversion, as illustrated in Fig. 3. The corresponding DSC curves for each of these measurements are shown in Figure S1. The experimental measurements are presented together with a fit to the empirical DiBenedetto's equation [53–55]:

$$\frac{(T_g - T_{g0})}{(T_{g\infty} - T_{g0})} = \frac{\lambda\alpha}{(1-(1-\lambda)\alpha)}, \tag{8}$$

where, Tg_∞ represents the glass transition temperature of the fully cured resin, and Tg_0 is the glass transition at zero degrees of cure. λ is a fitting parameter ranging between 0 and 1.

The DiBenedetto fit gives λ = 0.64 with an R^2 value of 0.998. It should be noted that for many epoxy resins the λ value is between 0.5 and 0.6 [56] and a λ value of 0.57 has been reported for an epoxy vitrimer [52]. Thus, our resin has a slightly higher Tg than the typical values reported for epoxy-based resins.

Besides vitrification, gelation is the other major event affecting the processing of thermosets. We have determined the time to gelation from the crossover point of the storage and loss moduli in rheological time sweep experiments conducted under isothermal conditions at four different temperatures (Fig. 4).

Following the methodology described in Section 2.2 we have determined the degree of cure at gelation, α_{gel}, for each of the 4 experiments. The time to gelation along with the calculated degree of cure based on isoconversional predictions, is summarized in Table 2.

We obtain an approximately constant value of $\alpha_{gel} = 0.79$. In step-growth systems, gel formation occurs typically at degrees of conversion between 0.5 and 0.8 [57]. In stoichiometric mixtures of diepoxy-diamine systems, the Flory–Stockmayer model predicts an $\alpha_{gel} = 0.577$ and most experimental results approximate 0.6 [58]. Thus, the gel point of our vitrimer is significantly delayed compared to typical diepoxy-diamine systems. Actually, high gel conversions have been described when deviations from the ideal stepwise cross-linking reaction occur [59,60].

Alternatively, gelation kinetics can be characterized by fitting the results presented in Table 2 to an Arrhenius temperature dependence.

$$\ln t_{gel}(T) = A - E/RT. \tag{9}$$

Fig. 5 depicts the logarithm of the gel time plotted against the reciprocal of the curing temperature. From the slope of the linear fit, we determine an activation energy of 58.5 kJ/mol, which agrees with the apparent activation energy obtained at α_{gel} from the isoconversional analysis, 55.2 kJ/mol (Fig. 2).

3.2. Stress relaxation kinetics

Reprocessing of vitrimers is governed by the exchange reaction between their dynamic bonds and manifested by a relaxation of the stress state. Fig. 6 shows the stress relaxation analysis of the epoxy vitrimer. All isothermal tests performed in the studied temperature range reveal the expected decay in the relaxation modulus, σ, above the transition temperature where the exchangeable reaction happens rapidly. This is known as the topological freezing transition temperature (T_v) [61].

For the kinetic analysis we assume that the degree of conversion of the exchange reaction is proportional to the applied load, where α = 0 when $\sigma = \sigma_0$, and α = 1 corresponds to a fully relaxed state:

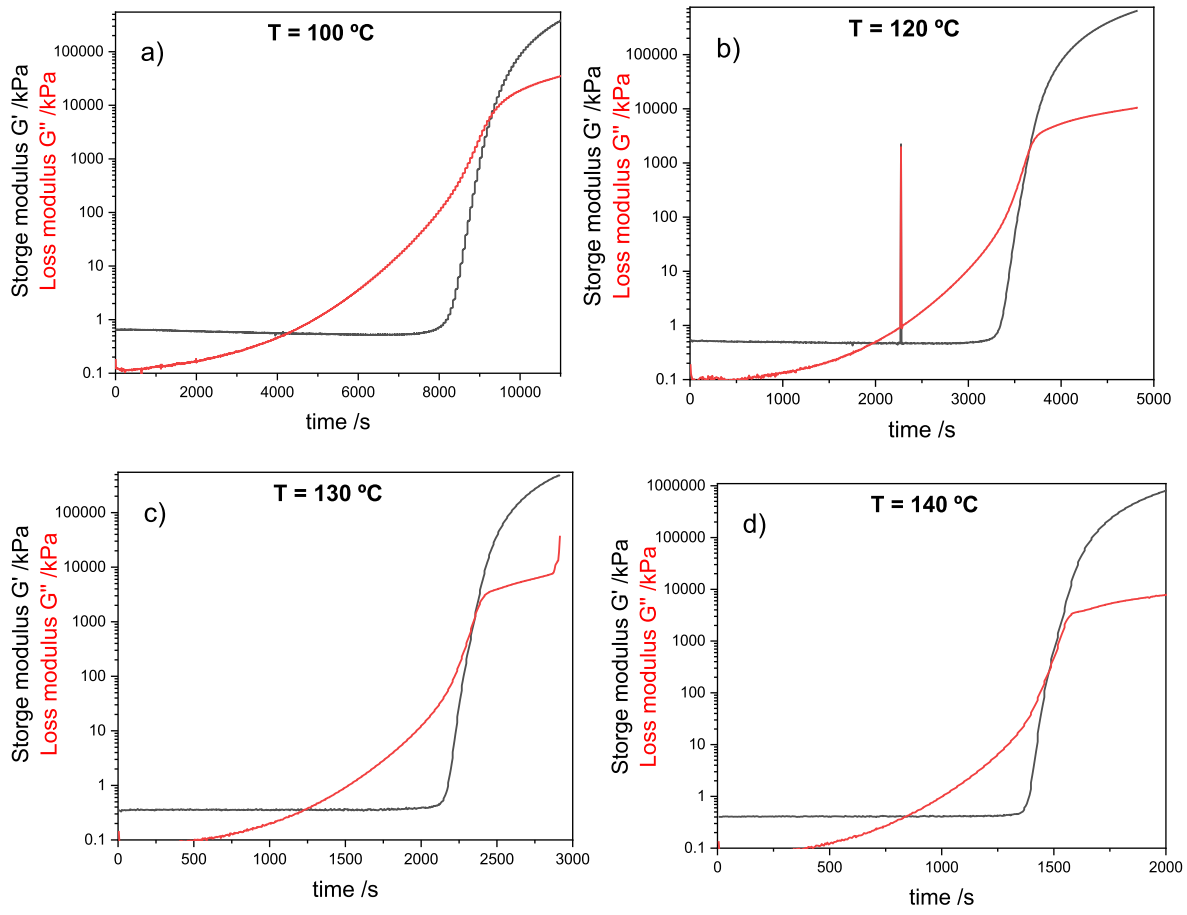

Fig. 4. Isothermal rheological time sweep experiments of the epoxy vitrimer. The spike in Fig. 4.b is an experimental artefact.

Table 2
– Gelation time at different temperatures and the corresponding degree of conversion determined from kinetic predictions.

Temperature	t_{gel} [s]	α_{gel}
100	9289.6	0.789
120	3659.4	0.794
130	2357.7	0.793
140	1479.9	0.781

$$\alpha(t) = \frac{\sigma_0 - \sigma(t)}{\sigma_0}. \quad (10)$$

Fig. 7 shows the result of applying Friedman's isoconversional method to the resulting $d\alpha/dt$ curves. The apparent activation energy of the process is close to 120 kJ/mol, increasing smoothly to 140 kJ/mol in the final stages of the process. To perform the Friedman isoconversional analysis we first need to calculate the time derivative of the DMA curves and the transformation rate is very sensitive to noise [62]. To overcome this problem and taking advantage of the fact that the DMA curves show a smooth evolution, we have first performed a cubic spline interpolation [32]. In addition, the sawtooth-like shape of the graphs in Fig. 7 is related to the fact that the DMA curves do not cover the entire α interval. As a result, the number of points used in the Friedman linear fit is not constant; every time this number changes there is a jump.

Commonly, stress relaxation kinetics have been characterized by fitting the characteristic stress relaxation time, τ*, defined as the time required to relax 63 % of the initial load, to an Arrhenius law [43,63,64]:

$$\ln\tau^*(T) = \ln\tau_0^* + E_\tau/RT, \quad (11)$$

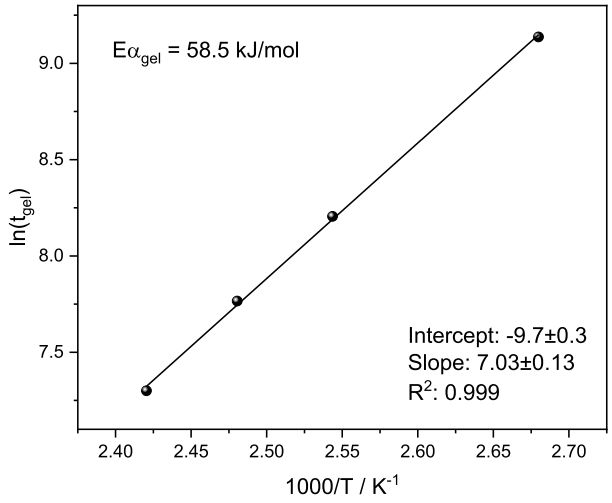

Fig. 5. Logarithm of the gel time plotted against the reciprocal of the curing temperature.

where, E_τ is the constant activation energy of the process and τ_0^* is a pre-exponential factor.

By applying this method, we found that E_τ is 105 kJ/mol (see the Supporting Information), which is in fairly agreement with the E_α values obtained in our isoconversional analysis.

Extrapolation of this same fit, in combination with Maxwell's relation (Eq. (12)), is commonly used to determine T_v as the threshold

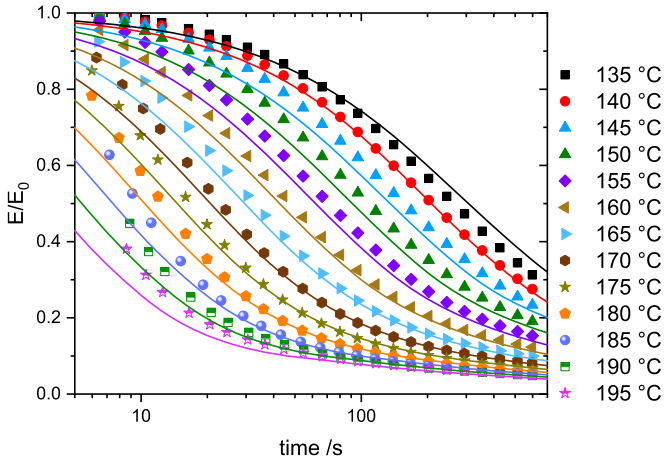

Fig. 6. - Symbols: Experimental stress relaxation curves at different temperatures. Lines: Simulations based on isoconversional analysis.

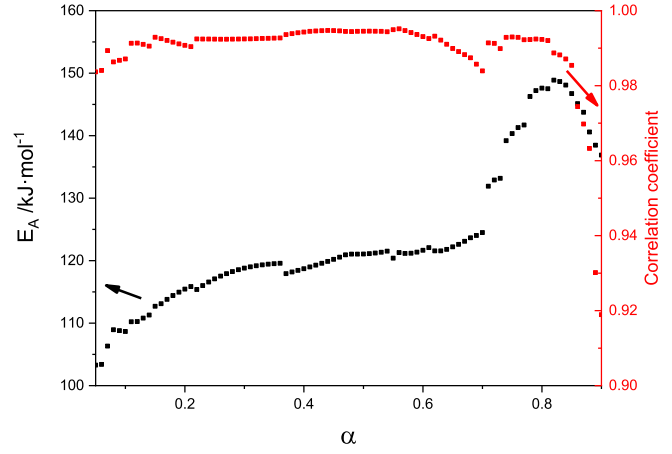

Fig. 7. Apparent activation energy of the stress relaxation effect determined using Friedman isoconversional analysis (left-side axis), along with the correlation coefficient of the method (right-side axis).

temperature at which the viscosity reaches a value of 10^{12} Pa [63–65]:

$$\eta = G{\cdot}\tau^{*}, \tag{12}$$

where the shear modulus, G, was calculated from the tensile modulus as measured by DMA from the relation:

$$G = \sigma_0/(2(1+\nu)), \tag{13}$$

where ν is the Poisson's ratio. We have considered that $\nu = 0.5$, i.e., the Poisson's ratio commonly used for rubbers.

This approach results in a T_v of 68.8 °C. It is important to note that this temperature is lower than the glass transition temperature of the fully cured resin. Therefore, the onset temperature at which the dynamic bond exchange reaction becomes significant is Tg_∞.

In Fig. 6 we have superimposed the predictions of the isoconversional analysis on the experimental data. The method shows notable inaccuracies for very short times, particularly at low degrees of transformation. These discrepancies are partly magnified when representing the data in logarithmic scale and are particularly pronounced when predicting the kinetic behavior for temperatures close to the limits of the range explored, i.e., 135 and 195 °C. Conversely, the predictions fit closely to experiments at longer times and intermediate temperatures.

It should be noted that we have fitted the relaxation data to the stretched exponential and Maxwell models [66–68], these analyses are detailed in the supplementary information. The Maxwell model is only able to fit the data over a narrow temperature range, from 130 to 155 °C. As for the stretched exponential model, we obtain a reasonable fit over a much wider temperature range, but the exponent β evolves from 0.824 to 0.292 while it is expected to be approximately constant. Thus, for the vitrimer analyzed, none of these models is able to provide a reliable description of the stress relaxation kinetics. Therefore, the isoconversional approach proposed here is an interesting alternative when the classical models do not provide a reliable description of the relaxation kinetics.

3.3. Thermal degradation kinetics

Prolonged exposure of the vitrimer to excessive temperatures will compromise its thermal stability during processing and reprocessing. It is therefore necessary to understand the kinetics of thermal degradation in order to prevent any deterioration in mechanical properties. We carried out a characterization of the vitrimer degradation based on the thermally driven mass loss criterion using non-isothermal TGA. In Fig. 8 we have plotted the normalized TGA curves and their time derivative (dTG) obtained when the vitrimer was heated at different heating rates.

All the thermograms obtained in air show clearly two main dTG peaks, starting at around 250 °C and continuing beyond temperatures of 550 °C. The initial stage, which marks the onset of degradation, is consistent with the expected thermal stability of the disulfide bonds [13], as noted above. While, in practical terms, only the first stage holds significance, both processes must be considered as a whole for the application of isoconversional methods. This is because it is imperative to define a physical state common to all experiments corresponding to 100 % process conversion. Since it is not possible to separate the two

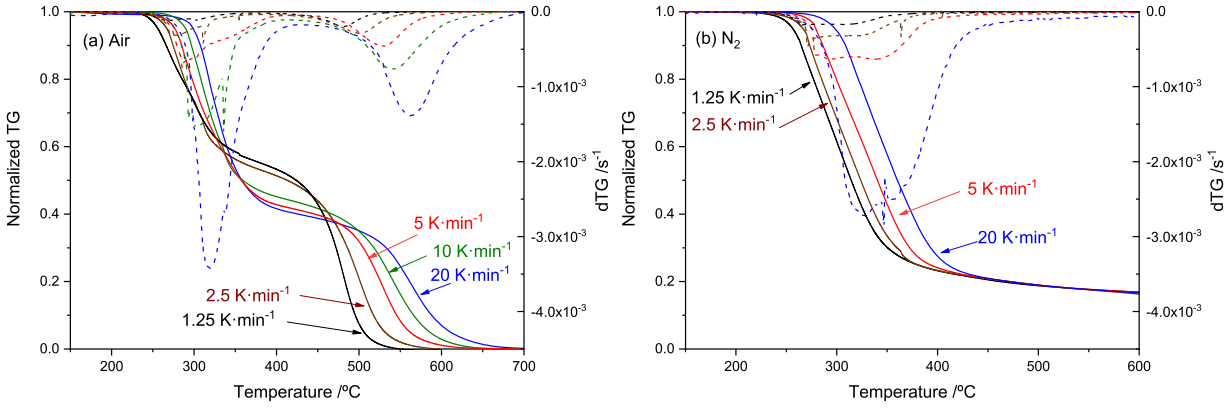

Fig. 8. Dynamic TG analysis of the vitrimer heated at different rates. Flowing gas: (a) synthetic air and (b) N_2.

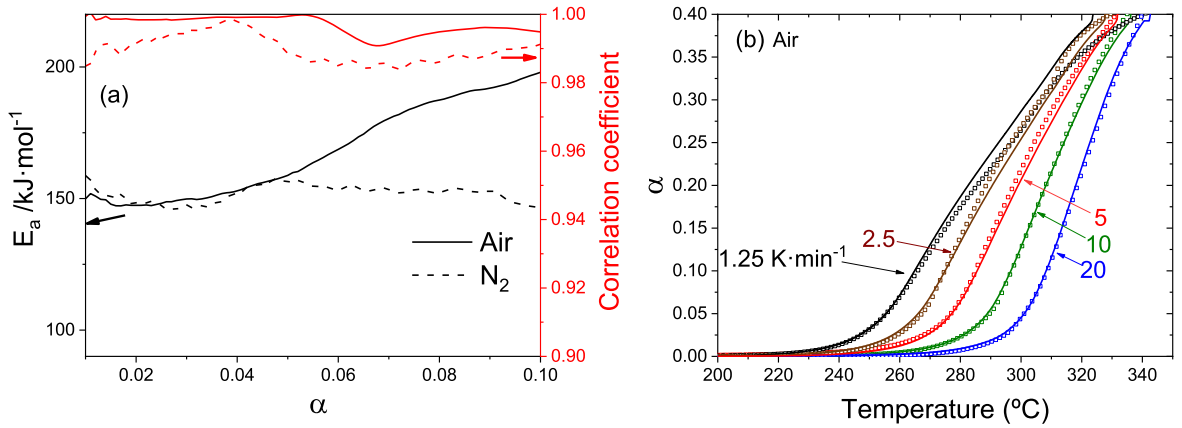

Fig. 9. (a) Apparent activation energy of the decomposition reaction determined using Friedman isoconversional analysis (left-side axis), along with the correlation coefficient of the related linear fit (right-side axis) for the experiments performed in synthetic air (solid line) and in N_2 (dashed line). (b) Degree of decomposition determined from the experiments shown in *Fig. 8*.a (symbols) and the corresponding prediction using *Eq. (7)* (solid lines).

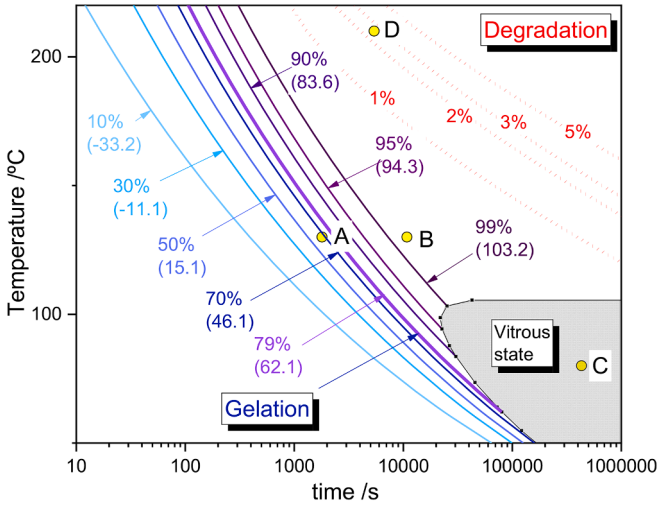

Fig. 10. - Processing map: Solid lines depict the isoconversional glass transition lines corresponding to advancing degrees of cure. (In brackets, the corresponding glass transition temperature). The gelation isoconversional line is in bold. Red dotted lines represent the time below which a tolerable degradation degree of 1 %, 2 %, 3 %, and 5 % is not exceeded. The grey dashed area indicates the conditions in which the vitrimer is in a vitreous state.

stages due to overlapping, we have defined total degradation as being achieved when the mass is virtually zero. Fig. 9.a shows the dependence of the apparent activation energy on the degree of degradation determined by using Friedman's method on the experiments outlined in Fig. 8. From the self-consistency test shown in Fig. 9.b, we can state that the kinetic analysis correctly predicts the evolution of the constant heating experiments up to a degree of conversion of 0.4, above this degree of degradation the predictions clearly deviate from the measured evolution. However, to construct the processing map it is sufficient to correctly predict the kinetics up to a degradation degree of 0.05. Moreover, in the $0.01 < \alpha < 0.1$ range, E_α evolve from around 150 kJ/mol initially to approximately 200 kJ/mol. This correlation is supported by a robust fit with a high correlation coefficient (Fig. 9.a, right side axe) and, again, is consistent with [13].

Both the apparent activation energies and the shapes of the TG curves obtained in N_2 and air in the early stages of the decomposition are similar. This similarity arises from the fact that the decomposition is initiated by the thermal decomposition of the disulphide hardener [13].

3.4. Processing map

The kinetics of curing and degradation have been summarized in Fig. 10 in the form of a TTT diagram that serves as a processing map. Based on predictions derived from the isoconversional analysis in Sections 3.1 and 3.3, the diagram illustrates the time dependence of these phenomena under isothermal conditions over the temperature range from 50 to 220 °C. The successive solid contour lines in the diagram reflect progressively higher degrees of cure and are correlated with the glass transition temperature by the DiBenedetto fit. This plot takes into account the maximum conversion achievable before vitrification, α_{max}, which delimits the zone in which the vitrimer is in the glassy state. We have also highlighted in bold the degree of conversion that marks the gel transition, α_{gel}. The red dotted lines take into account the degradation kinetics and establish several degrees of degradation in the range of 1 to 5 %. Integrating these different transformations into a unified plot unveils the window of processing conditions (temperature-time) where both degradation and vitrification are avoided, thus ensuring attaining the desired degree of cure.

To validate the reliability of the diagram in its different regions, we performed tests designed to explore the conditions that lead to the different possible states of the resin. For instance, samples A and B were treated at 130 °C for 30 min and 3 h, respectively, aiming at cure degrees below and above gelation. Under these conditions, sample A should have reached an α of 58 %, while sample B should have reached an α of 94%. These degrees of conversion correspond to Tg values of 36.6 °C and 93.8 °C, respectively. This is in reasonably good agreement with the measured values of 34.2 °C and 99.6 °C obtained by calorimetric measurements (see Figs. 11a and b).

Sample C was heated at 80 °C for five days, aiming at the vitrification region. An indirect validation that a sample has vitrified is the occurrence of physical ageing, a direct consequence of the metastable nature of glassy amorphous polymers [69]. Physical ageing manifests itself as an endothermic peak at a temperature that depends on the ageing time [70,71]. Sample C shows this characteristic relaxation event upon heating in a DSC scan (Fig. 11.c). The onset of relaxation is marked by a fictive temperature [71] at around 100 °C, dictated by the structure of the glass. Predicting the peak shift with ageing requires an understanding of the relaxation kinetics in the glass transition region [71], which is beyond the scope of this work.

Finally, sample D was treated at 210 °C for 1.5 h and lies in the region where significant degradation is expected. Specifically, this sample was expected to experience a loss of 2 to 3 % of its initial mass. A thermogravimetric experiment, replicating these conditions confirmed our prediction with a measured mass loss of 2.7 % (Fig. 12). Although the measured and predicted degradation are in excellent agreement, a very

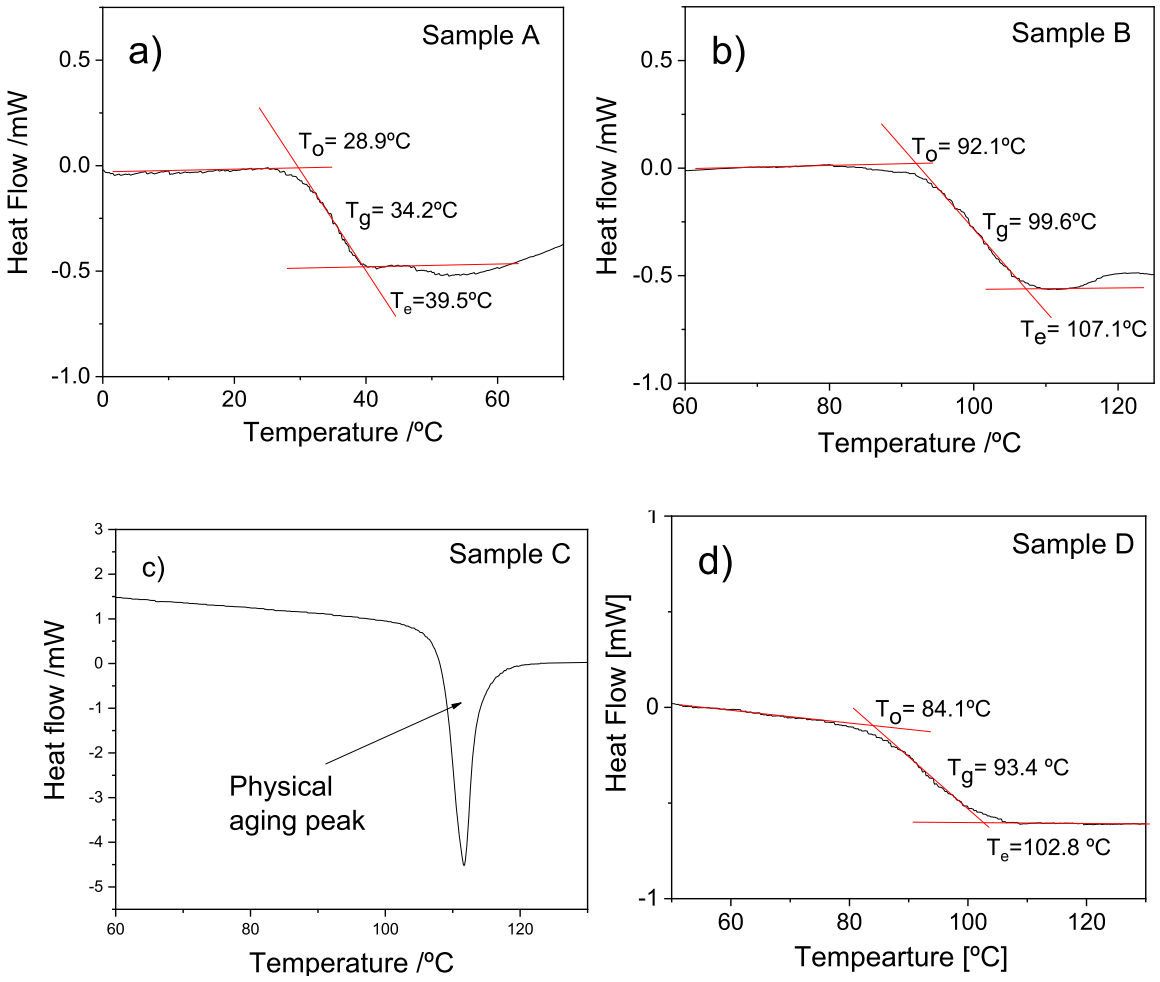

Fig. 11. Calorimetric measurements performed at 10 K/min, corresponding to samples treated under conditions labeled as A, B, C and D in Fig. 10.

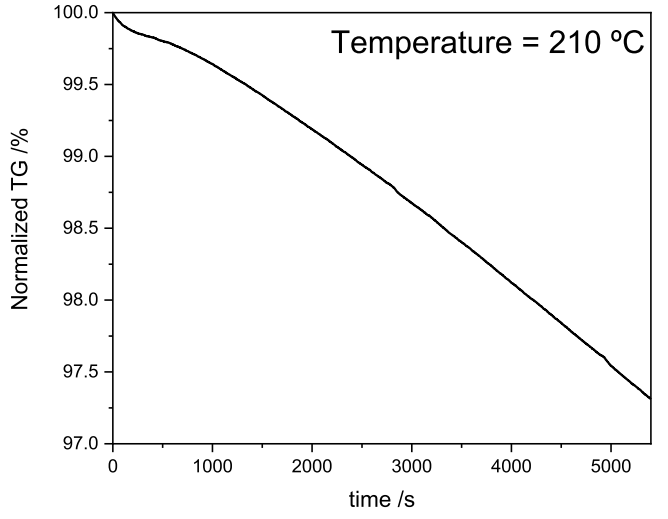

Fig. 12. – Thermogravimetric experiment corresponding to condition D in Fig. 10.

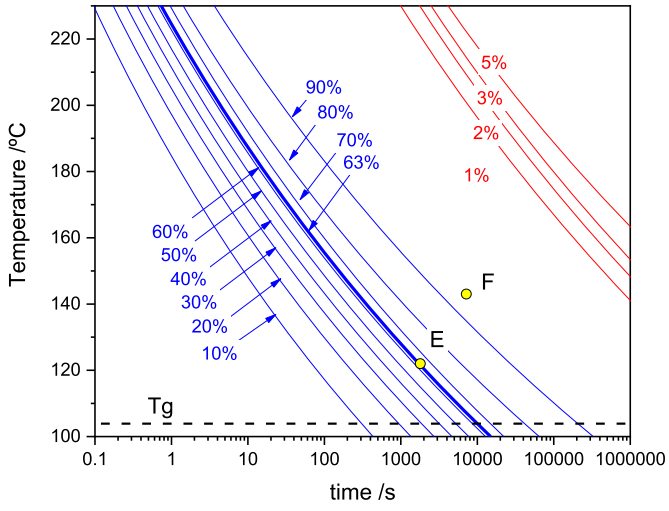

Fig. 13. Reprocessing map of the epoxy vitrimer: Blue solid lines show the time required to relax stress by several degrees. Red lines show the time below which a tolerable degradation degree of 1 %, 2%, 3 % and 5 % is not exceeded.

accurate prediction for the early stages of degradation cannot be expected due to the small mass losses measured by the TG and the accuracy of the kinetic model. However, the aim of the transformation diagram is not to accurately predict degradation in the early stages, but to have an estimate of the time-temperature conditions to avoid thermal degradation. Furthermore, we observed a Tg of 93.4 °C, which is about 10 °C below Tg_∞, despite an extended processing time well beyond the completion of curing. This decrease in Tg is also indicative of the material experiencing degradation.

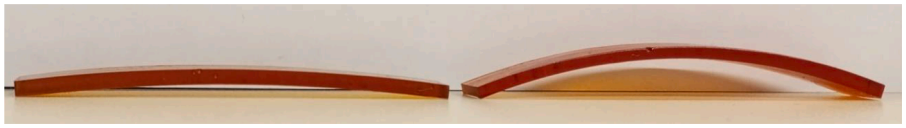

Fig. 14. Deformed cupons after the second reprocessing step. Left) Sample E, Right) Sample F.

3.5. Reprocessing map

We have generated a diagram analogous to the processing map for reprocessing vitrimers, where the role of the curing reaction is taken over by the dynamic bond exchange reaction (Fig. 13). This plot maintains the same degradation criteria but omits the glassy state region, since the temperature range of interest is above the $T_{g\infty}$. In Fig. 13, the solid lines describe contours of constant degree of conversion for the stress relaxation kinetics described in Section 3.2. The diagram shows the time required for relaxation expanding from 10 to 90 % of the initial stress at 10 % intervals. We have also included, in bold, the classical criterion (τ^*) corresponding to a stress relaxation of 63 %. The interpretation of Fig. 13 thus reveals a clear range of safe conditions, indicating that thermoforming is feasible without significant degradation. Moreover, this novel representation also offers valuable insights into the residual stress state that persists after post-reprocessing; thus going beyond the considerations made by other researchers to date. This is of significant importance, as an excess of residual stresses has the potential to diminish the load-carrying capacity, weaken the strength, and shorten the service life of the composite material in question [72,73].

Residual stresses also pose a significant obstacle to achieving precise geometrical tolerances. For instance, angled parts may experience 'spring-in', causing difficulties during assembly with other components. This issue, commonly observed in the processing of composite material [74,75], extends to the thermoforming of vitrimers. In this context, the reprocessing map can be utilized to ensure the quality of reshaping.

To underscore the value of the reprocessing map, we follow a procedure that unfolds in two stages. The first stage consist in reprocessing two flat samples, each measuring $80\times30\times3$ mm^3, into a curved mold (Figure S7) under conditions E and F as indicated in Fig. 13. For this purpose, the sample is immersed in a silicone bath held at a constant temperature for a designated period. After the completion of the reprocessing stage, the sample is cooled to room temperature and then extracted from the mold. As a result of this first stage the sample retain the curvature of the mold (Fig. S8) and accumulate residual stress due to their deformation. Based on our predictions, during this first stage, the sample reprocessed under conditions E (122 °C for 30 min) only relaxes 63 % of the stresses, a relaxation level that is commonly used to determine the characteristic reshaping time of vitrimers [76]. On the other hand, sample F is treated at a higher temperature and for a longer time (143 °C for 2 h) with the aim to relax well beyond the 90 % of the stresses induced by the mold.

At room temperature, the sample shape is partly maintained because it is in a glassy state, with the strain rate 'frozen'. However, if the sample is heated again above Tg, residual stresses would be relaxed and a partial recovery of the initial shape would take place. To confirm that the stress accumulated on the sample depends on the reprocessing conditions, we perform a second stage that consist of heating the sample outside the mold and above Tg. While sample E displays a pronounced spring-in effect, resulting in a final curvature much greater than that of the mold, sample F maintains its shape with minimal spring-in (Figure S9). A comparison of the final shape of the two reprocessed samples is shown in Fig. 14.

4. Conclusions

The kinetics of curing, degradation, and stress relaxation in a disulfide-containing epoxy vitrimer have been investigated using the Friedman isoconversional method. This complete characterization has been captured in the form of two TTT diagrams describing the primary reactions that take place during the processing and reprocessing of the resin.

We have shown that Friedman isoconversional analysis applied to dynamic calorimetric experiments is useful for predicting the evolution of the glass transition under isothermal conditions when the cure kinetics are controlled by the reaction. Furthermore, the predictions accurately describe resin gelation within the limits defined by the thermoanalytical data used to feed the model.

The decomposition behavior of the vitrimer studied, well described by isoconversional model in the first stages, suggests that its thermal stability is dictated by the stability of the disulfide bonds that give the vitrimer its ability to flow.

Finally, we have applied isoconversional analysis for the first time to characterize the kinetics of the stress relaxation in a vitrimer. The analysis yielded an apparent activation energy for the disulfide bond exchange reaction in the range of approximately 100–140 kJ/mol over the 10–90 % relaxation interval of the initial stresses. Predictions based on this kinetic characterization are in good agreement with the experimental results, especially for long reprocessing times.

CRediT authorship contribution statement

D. Sanchez-Rodriguez: Writing – original draft, Validation, Methodology, Investigation, Formal analysis, Conceptualization. **S. Zaidi:** Investigation, Formal analysis, Data curation. **L. Carreras:** Visualization, Supervision, Methodology, Investigation. **Alaitz Ruiz de Luzuriaga:** Writing – review & editing, Visualization, Resources, Investigation, Data curation, Conceptualization. **Alaitz Rekondo:** Writing – review & editing, Visualization, Resources, Investigation, Data curation, Conceptualization. **J. Costa:** Writing – review & editing, Visualization, Validation, Supervision, Funding acquisition, Conceptualization. **J. Farjas:** Writing – review & editing, Software, Methodology, Investigation, Funding acquisition, Formal analysis, Conceptualization.

Declaration of competing interest

The authors declare that they have no known competing financial interests or personal relationships that could have appeared to influence the work reported in this paper.

Data availability

Data will be made available on request.

Acknowledgments

The authors acknowledge AMADE and the GRMT project PID2021-126989OB-I00 financed by the Ministerio de Ciencia e Innovación, Spain). We also thank the support from the Catalan Government with project 2017SGR1378. D.S.R. acknowledges the support received from the Beatriu de Pinós Programme, and the Ministry of Research and Universities of the Catalan Government (Fellowship BP00069), and L.C. acknowledges the grant RYC2021-032171-I funded by MCIN/AEI/10.13039/501100011033 and by "European Union NextGenerationEU/PRTR". Open Access funding provided thanks to the CRUE-CSIC

agreement with Elsevier.

Supplementary materials

Supplementary material associated with this article can be found, in the online version, at doi:10.1016/j.tca.2024.179744.

References

[1] Polymer engineering science and viscoelasticity: an introduction, Characteristics, Applications and Properties of Polymers, Springer US, Boston, MA, 2008, pp. 55–97, https://doi.org/10.1007/978-0-387-73861-1_3.

[2] F.-L. Jin, S.-Y. Lee, S.-J. Park, Polymer matrices for carbon fiber-reinforced polymer composites, Carbon Lett. 14 (2013) 76–88, https://doi.org/10.5714/cl.2013.14.2.076.

[3] M.Y. Khalid, Z.U. Arif, W. Ahmed, H. Arshad, Recent trends in recycling and reusing techniques of different plastic polymers and their composite materials, Sustain. Mater. Technol. 31 (2022) e00382, https://doi.org/10.1016/j.susmat.2021.e00382.

[4] S. Kamarulzaman, Z.M. Png, E.Q. Lim, I.Z.S. Lim, Z. Li, S.S. Goh, Covalent adaptable networks from renewable resources: crosslinked polymers for a sustainable future, Chem 9 (2023) 2771–2816, https://doi.org/10.1016/j.chempr.2023.04.024.

[5] A. Ruiz De Luzuriaga, R. Martin, N. Markaide, A. Rekondo, G. Cabañero, J. Rodríguez, I. Odriozola, Epoxy resin with exchangeable disulfide crosslinks to obtain reprocessable, repairable and recyclable fiber-reinforced thermoset composites, Mater. Horiz. 3 (2016) 241–247, https://doi.org/10.1039/c6mh00029k.

[6] B. Krishnakumar, R.V.S.P. Sanka, W.H. Binder, V. Parthasarthy, S. Rana, N. Karak, Vitrimers: associative dynamic covalent adaptive networks in thermoset polymers, Chem. Eng. J. 385 (2020) 123820, https://doi.org/10.1016/j.cej.2019.123820.

[7] M. Guerre, C. Taplan, J.M. Winne, F.E. Du Prez, Vitrimers: directing chemical reactivity to control material properties, Chem. Sci. 11 (2020) 4855–4870, https://doi.org/10.1039/d0sc01069c.

[8] M. Capelot, M.M. Unterlass, F. Tournilhac, L. Leibler, Catalytic control of the vitrimer glass transition, ACS. Macro Lett. 1 (2012) 789–792, https://doi.org/10.1021/mz300239f.

[9] S. Zaidi, S. Thakur, D. Sanchez-rodriguez, R. Verdejo, J. Farjas, J. Costa, Optimal processing conditions of a bio-based epoxy synthesized from vanillyl alcohol, Polym. Degrad. Stab. 223 (2024) 110743, https://doi.org/10.1016/j.polymdegradstab.2024.110743.

[10] L.C. Chan, H.N. Naé, J.K. Gillham, Time-temperature–transformation (TTT) diagrams of high Tg epoxy systems: competition between cure and thermal degradation, J. Appl. Polym. Sci. 29 (1984) 3307–3327, https://doi.org/10.1002/app.1984.070291109.

[11] J.B. Enns, J.K. Gillham, P.M. Program, Time-temperature-transformation (TTT) cure diagram : modeling the cure behavior of thermosets below TGM, J. Appl. Polym. Sci. 28 (1983) 2567–2591.

[12] S. Huang, G. Zhang, W. Du, H. Chen, Construction of a TTT–η diagram of high–refractive polyurethane based on curing kinetics, Polymers (Basel) 13 (2021), https://doi.org/10.3390/polym13203474.

[13] D. Sanchez-Rodriguez, S. Zaidi, Y. Jahani, A. Ruiz de Luzuriaga, A. Rekondo, P. Maimi, J. Farjas, J. Costa, Processability and reprocessability maps for vitrimers considering thermal degradation and thermal gradients, Polym. Degrad. Stab. 217 (2023) 110543, https://doi.org/10.1016/j.polymdegradstab.2023.110543.

[14] C.K. Tziamtzi, K. Chrissafis, Optimization of a commercial epoxy curing cycle via DSC data kinetics modelling and TTT plot construction, Polymer 230 (2021), https://doi.org/10.1016/j.polymer.2021.124091.

[15] Q. Li, X. Li, Y. Meng, Curing of DGEBA epoxy using a phenol-terminated hyperbranched curing agent: cure kinetics, gelation, and the TTT cure diagram, Thermochim. Acta 549 (2012) 69–80, https://doi.org/10.1016/j.tca.2012.09.012.

[16] S. Sourour, M.R. Kamal, Differential scanning calorimetry of epoxy cure: isothermal cure kinetics, Thermochim. Acta 14 (1976) 41–59, https://doi.org/10.1016/0040-6031(76)80056-1.

[17] J. Wang, Q. Mao, Methodology based on the PVT behavior of polymer for injection molding, Adv. Polym. Technol. 32 (2012) 474–485, https://doi.org/10.1002/adv.

[18] A.A. Skordos, I.K. Partridge, Cure kinetics modeling of epoxy resins using a non-parametric numerical procedure, Polym. Eng. Sci. 41 (2001) 793–805, https://doi.org/10.1002/pen.10777.

[19] S. Vyazovkin, D. Achilias, X. Fernandez-Francos, A. Galukhin, N. Sbirrazzuoli, ICTAC kinetics committee recommendations for analysis of thermal polymerization kinetics, Thermochim. Acta 714 (2022) 179243, https://doi.org/10.1016/j.tca.2022.179243.

[20] S. Vyazovkin, A.K. Burnham, L. Favergeon, N. Koga, E. Moukhina, L.A. Pérez-Maqueda, N. Sbirrazzuoli, ICTAC Kinetics committee recommendations for analysis of multi-step kinetics, Thermochim. Acta 689 (2020) 178597, https://doi.org/10.1016/j.tca.2020.178597.

[21] S. Vyazovkin, N. Sbirrazzuoli, Mechanism and kinetics of epoxy−amine cure studied by differential scanning calorimetry, Macromolecules. 29 (1996) 1867–1873, https://doi.org/10.1021/ma951162w.

[22] M. Vafayan, M. Hosain Beheshty, M.H.R. Ghoreishy, H. Abedini, Advanced integral isoconversional analysis for evaluating and predicting the kinetic parameters of the curing reaction of epoxy prepreg, Thermochim. Acta 557 (2013) 37–43, https://doi.org/10.1016/j.tca.2013.01.035.

[23] P. Budrugeac, A. Cucos, R. Dascălu, C. Paraschiv, S. Mitrea, B.-G. Sbarcea, The use of thermal analysis methods for predicting the thermal endurance of an epoxy resin used as electrical insulator, J. Therm. Anal. Calorim. 146 (2021) 1791–1801, https://doi.org/10.1007/s10973-020-10156-5.

[24] J.D. Thanki, P.H. Parsania, Dynamic DSC curing kinetics and thermogravimetric study of epoxy resin of 9,9′-bis(4-hydroxyphenyl)anthrone-10, J. Therm. Anal. Calorim. 130 (2017) 2145–2156, https://doi.org/10.1007/s10973-017-6761-y.

[25] G. Gerami, R. Bagheri, R. Darvishi, Investigation of isothermal and dynamic cure kinetics of epoxy resin/nadic methyl anhydride/dicyandiamide by differential scanning calorimetry (DSC), J. Therm. Anal. Calorim. 137 (2019) 575–582, https://doi.org/10.1007/s10973-018-7961-9.

[26] G. Wuzella, A.R. Mahendran, C. Beuc, H. Lammer, Isoconversional cure kinetics of a novel thermosetting resin based on linseed oil, J. Therm. Anal. Calorim. 142 (2020) 1055–1071, https://doi.org/10.1007/s10973-020-09529-7.

[27] M. Jouyandeh, S.M.R. Paran, A. Jannesari, D. Puglia, M.R. Saeb, Protocol for nonisothermal cure analysis of thermoset composites, Prog. Org. Coat. 131 (2019) 333–339, https://doi.org/10.1016/j.porgcoat.2019.02.040.

[28] A. Redmann, P. Oehlmann, T. Scheffler, L. Kagermeier, T.A. Osswald, Thermal curing kinetics optimization of epoxy resin in Digital Light Synthesis, Addit. Manuf. 32 (2020) 101018, https://doi.org/10.1016/j.addma.2019.101018.

[29] M. Joseph D., P.R. Bruce (Eds.), Thermal Analysis of Polymers, John Wiley & Sons, Hoboken, NJ, USA, 2009, https://doi.org/10.1002/9780470423837.

[30] S. Vyazovkin, Thermal Analysis, Anal. Chem. 82 (2010) 4936–4949, https://doi.org/10.1021/ac100859s.

[31] S. Vyazovkin, C.A. Wight, Isothermal and Nonisothermal reaction kinetics in solids: in search of ways toward consensus, J. Phys. Chem. A 101 (1997) 8279–8284, https://doi.org/10.1021/jp971889h.

[32] J. Farjas, P. Roura, Isoconversional analysis of solid state transformations: a critical review. Part II. Complex transformations, J. Therm. Anal. Calorim. 105 (2011) 767–773, https://doi.org/10.1007/s10973-011-1447-3.

[33] S. Vyazovkin, Activation energies and temperature dependencies of the rates of crystallization and melting of polymers, Polymers (Basel) 12 (2020), https://doi.org/10.3390/POLYM12051070.

[34] S. Vyazovkin, A.K. Burnham, J.M. Criado, L.A. Pérez-Maqueda, C. Popescu, N. Sbirrazzuoli, ICTAC kinetics committee recommendations for performing kinetic computations on thermal analysis data, Thermochim. Acta 520 (2011) 1–19, https://doi.org/10.1016/j.tca.2011.03.034.

[35] S. Vyazovkin, Comments on multiple publications reporting single heating rate kinetics, Appl. Organomet. Chem. 37 (2023) e6929, https://doi.org/10.1002/aoc.6929.

[36] W. Press, B. Flannery, S. Teukolky, W. Vetterling, Numerical Recipes in C: the Art of Scientific Computing, Cambridge University Press, Cambridge, 1994.

[37] J. Farjas, P. Roura, Isoconversional analysis of solid-state transformations: a critical review. Part III. Isothermal and non isothermal predictions, J. Therm. Anal. Calorim. 109 (2012) 183–191, https://doi.org/10.1007/s10973-011-1642-2.

[38] B. Roduit, P. Folly, B. Berger, J. Mathieu, A. Sarbach, H. Andres, M. Ramin, B. Vogelsanger, Evaluating SADT by advanced kinetics-based simulation approach, J. Therm. Anal. Calorim. 93 (2008) 153–161, https://doi.org/10.1007/s10973-007-8865-2.

[39] S. Rasi, P. Roura-Grabulosa, J. Farjas, Application of thermal analysis and kinetic predictions to YBCO films prepared by chemical solution deposition methods, J. Therm. Anal. Calorim. 142 (2020) 2077–2086, https://doi.org/10.1007/s10973-020-10103-4.

[40] E.G. Hanna, K. Younes, S. Amine, R. Roufayel, Rheology and unsupervised learning, (2023).

[41] T.A. Instruments, Gelation kinetics from rheological experiments, TA Instruments Technical Notes - RH103 (n.d.).

[42] E.A. Turi, Thermal characterisation of polymeric materials, Polym. Test. 5 (1997) 523–524.

[43] A. Ruiz de Luzuriaga, G. Solera, I. Azcarate-Ascasua, V. Boucher, H.J. Grande, A. Rekondo, Chemical control of the aromatic disulfide exchange kinetics for tailor-made epoxy vitrimers, Polymer 239 (2022) 124457, https://doi.org/10.1016/j.polymer.2021.124457.

[44] D. Sánchez-Rodríguez, H. Eloussifi, J. Farjas, P. Roura, M. Dammak, Thermal gradients in thermal analysis experiments: criterions to prevent inaccuracies when determining sample temperature and kinetic parameters, Thermochim. Acta 589 (2014), https://doi.org/10.1016/j.tca.2014.05.001.

[45] S. Swier, B. Van Mele, Reaction thermodynamics of amine-cured epoxy systems: validation of the enthalpy and heat capacity of reaction as determined by modulated temperature differential scanning calorimetry, J. Polym. Sci. B Polym. Phys. 41 (2003) 594–608, https://doi.org/10.1002/polb.10413.

[46] J.M. Barton, The Application of Differential Scanning Calorimetry (DSC) to the Study of Epoxy Resin Curing Reactions BT - Epoxy Resins and Composites I, Springer Berlin Heidelberg, Berlin, Heidelberg, 1985, pp. 111–154.

[47] B.A. Rozenberg, Kinetics, Thermodynamics and Mechanism of Reactions of Epoxy Oligomers With Amines BT - Epoxy Resins and Composites II, Springer Berlin Heidelberg, Berlin, Heidelberg, 1986, pp. 113–165. K. Dušek.

[48] D. Lascano, L. Quiles-Carrillo, R. Balart, T. Boronat, N. Montanes, Kinetic analysis of the curing of a partially biobased epoxy resin using dynamic differential scanning calorimetry, Polymers (Basel) 11 (2019), https://doi.org/10.3390/polym11030391.

[49] N. Sbirrazzuoli, S. Vyazovkin, A. Mititelu, C. Sladic, L. Vincent, A study of epoxy-amine cure kinetics by combining isoconversional analysis with temperature

modulated DSC and dynamic rheometry, Macromol. Chem. Phys. 204 (2003) 1815–1821, https://doi.org/10.1002/macp.200350051.
[50] S. Vyazovkin, N. Sbirrazzuoli, Mechanism and kinetics of epoxy-amine cure studied by differential scanning calorimetry, Macromolecules 29 (1996) 1867–1873, https://doi.org/10.1021/ma951162w.
[51] N. Sbirrazzuoli, Interpretation and physical meaning of kinetic parameters obtained from isoconversional kinetic analysis of polymers, Polymers (Basel) 12 (2020), https://doi.org/10.3390/POLYM12061280.
[52] F.I. Anagwu, A.A. Skordos, Cure kinetics, glass transition advancement and chemo-rheological modelling of an epoxy vitrimer based on disulphide metathesis, Polymer 288 (2023) 126427, https://doi.org/10.1016/j.polymer.2023.126427.
[53] A.T. DiBenedetto, Prediction of the glass transition temperature of polymers: a model based on the principle of corresponding states, J. Polym. Sci. B Polym. Phys. 25 (1987) 1949–1969, https://doi.org/10.1002/polb.1987.090250914.
[54] A.T. Dibenedetto, L. Dilandro, Correlation of glass transition temperature and molecular weight: a model based on the principle of corresponding states, J. Polym. Sci. B Polym. Phys. 27 (1989) 1405–1417, https://doi.org/10.1002/polb.1989.090270703.
[55] J.P. Pascault, R.J.J. Williams, Relationships between glass transition temperature and conversion - Analyses of limiting cases, Polym. Bullet. 24 (1990) 115–121, https://doi.org/10.1007/BF00298330.
[56] J.P. Pascault, R.J.J. Williams, Glass transition temperature versus conversion relationships for thermosetting polymers, J. Polym. Sci. B Polym. Phys. 28 (1990) 85–95, https://doi.org/10.1002/polb.1990.090280107.
[57] R.P. Chartoff, J.D. Menczel, S.H. Dillman, Dynamic mechanical analysis (DMA). Thermal Analysis of Polymers, 2009, pp. 387–495, https://doi.org/10.1002/9780470423837.ch5.
[58] R.J.J. Pascault, J.-P. Sautereau, H. Verdu, J. Williams, Thermosetting Polymers, 1st ed., CRC press, 2002 https://doi.org/10.1201/9780203908402.
[59] Y. Tanaka, J.L. Stanford, R. Stepto, Interpretation of gel points of an epoxy-amine system including ring formation and unequal reactivity: measurements of gel points and analyses on ring structures, Macromolecules 45 (2012) 7197–7205, https://doi.org/10.1021/ma3009838.
[60] L. Matějka, Amine cured epoxide networks: formation, structure, and properties, Macromolecules 33 (2000) 3611–3619, https://doi.org/10.1021/ma991831w.
[61] Y. Yang, S. Zhang, X. Zhang, L. Gao, Y. Wei, Y. Ji, Detecting topology freezing transition temperature of vitrimers by AIE luminogens, Nat. Commun. 10 (2019) 3165, https://doi.org/10.1038/s41467-019-11144-6.
[62] A. Ortega, A simple and precise linear integral method for isoconversional data, Thermochim. Acta 474 (2008) 81–86, https://doi.org/10.1016/j.tca.2008.05.003.
[63] M. Guerre, C. Taplan, R. Nicolaÿ, J.M. Winne, F.E. Du Prez, Fluorinated vitrimer elastomers with a dual temperature response, J. Am. Chem. Soc. 140 (2018) 13272–13284, https://doi.org/10.1021/jacs.8b07094.
[64] Y. Nishimura, J. Chung, H. Muradyan, Z. Guan, Silyl ether as a robust and thermally stable dynamic covalent motif for malleable polymer design, J. Am. Chem. Soc. 139 (2017) 14881–14884, https://doi.org/10.1021/jacs.7b08826.
[65] G. Lopez, L. Granado, G. Coquil, A. Lárez-Sosa, N. Louvain, B. Améduri, Perfluoropolyether (PFPE)-Based vitrimers with ionic conductivity, Macromolecules 52 (2019) 2148–2155, https://doi.org/10.1021/acs.macromol.8b02493.
[66] X. Chen, L. Li, T. Wei, D.C. Venerus, J.M. Torkelson, Reprocessable polyhydroxyurethane network composites: effect of filler surface functionality on cross-link density recovery and stress relaxation, ACS. Appl. Mater. Interfaces 11 (2019) 2398–2407, https://doi.org/10.1021/acsami.8b19100.
[67] J.C. Hooker, J.M. Torkelson, Coupling of probe reorientation dynamics and rotor motions to polymer relaxation as sensed by second harmonic generation and fluorescence, Macromolecules 28 (1995) 7683–7692, https://doi.org/10.1021/ma00127a014.
[68] L. Li, X. Chen, J.M. Torkelson, Reprocessable polymer networks via thiourethane dynamic chemistry: recovery of cross-link density after recycling and proof-of-principle solvolysis leading to monomer recovery, Macromolecules 52 (2019) 8207–8216, https://doi.org/10.1021/acs.macromol.9b01359.
[69] S.G. Nunes, R. Joffe, N. Emami, P. Fernberg, S. Saseendran, A. Esposito, S. C. Amico, J. Varna, Physical aging effect on viscoelastic behavior of polymers, Compos. Part C: Open Access 7 (2022) 100223, https://doi.org/10.1016/j.jcomc.2021.100223.
[70] M. Song, Modulated differential scanning calorimetry observation of physical ageing in polymers, J. Therm. Anal. Calorim. 63 (2001) 699–707, https://doi.org/10.1023/A:1010131802572.
[71] S. Montserrat, Y. Calventus, J.M. Hutchinson, Physical aging of thermosetting powder coatings, Prog. Org. Coat. 55 (2006) 35–42, https://doi.org/10.1016/j.porgcoat.2005.10.005.
[72] M.W. Joosten, S. Agius, T. Hilditch, C. Wang, Effect of residual stress on the matrix fatigue cracking of rapidly cured epoxy/anhydride composites, Compos. Part a Appl. Sci. Manuf. 101 (2017) 521–528.
[73] H. Wang, Effect of spring-in deviation on fatigue life of composite elevator assembly, Appl. Compos. Mater. (Dordr) 25 (2018) 1357–1367.
[74] C. Albert, G. Fernlund, Spring-in and warpage of angled composite laminates, Compos. Sci. Technol. 62 (2002) 1895–1912.
[75] B. Wang, S. Fan, J. Chen, W. Yang, W. Liu, Y. Li, A review on prediction and control of curing process-induced deformation of continuous fiber-reinforced thermosetting composite structures, Compos. Part a Appl. Sci. Manuf. 165 (2023) 107321.
[76] F. Meng, M.O. Saed, E.M. Terentjev, Rheology of vitrimers, Nat. Commun. 13 (2022), https://doi.org/10.1038/s41467-022-33321-w.